0022-3565/11/3373-766–774$25.00
THE JOURNAL OF PHARMACOLOGY AND EXPERIMENTAL THERAPEUTICS
Vol. 337, No. 3
177790/3689943
Printed in U.S.A.

JPET 337:766–774, 2011

Inhibitory Effects of Antivascular Endothelial Growth Factor Strategies in Experimental Dopamine-Resistant Prolactinomas[S]

Guillermina María Luque, Maria Ines Perez-Millán, Ana Maria Ornstein, Carolina Cristina, and Damasia Becu-Villalobos

Instituto de Biología y Medicina Experimental, Consejo Nacional de Investigaciones Científicas y Técnicas, Buenos Aires, Argentina (G.M.L., M.I.P.-M., A.M.O., D.B.-V.); and Universidad Nacional del Noroeste de la Provincia de Buenos Aires, Junín, Buenos Aires, Argentina (C.C.)

Received December 6, 2010; accepted March 14, 2011

ABSTRACT

Prolactin-secreting adenomas are the most frequent type among pituitary tumors, and pharmacological therapy with dopamine agonists remains the mainstay of treatment. But some adenomas are resistant, and a decrease in the number or function of dopamine D2 receptors (D2Rs) has been described in these cases. D2R knockout [*Drd2*(−/−)] mice have chronic hyperprolactinemia and pituitary hyperplasia and provide an experimental model for dopamine agonist-resistant prolactinomas. We described previously that disruption of D2Rs increases vascular endothelial growth factor (VEGF) expression. We therefore designed two strategies of antiangiogenesis using prolactinomas generated in *Drd2*(−/−) female mice: direct intra-adenoma mVEGF R1 (Flt-1)/Fc chimera (VEGF-TRAP) injection for 3 weeks [into subcutaneously transplanted pituitaries from *Drd2*(−/−) mice] and systemic VEGF neutralization with the specific monoclonal antibody G6-31. Both strategies resulted in substantial decrease of prolactin content and lactotrope area, and a reduction in tumor size was observed in in situ prolactinomas. There were significant decreases in vascularity, evaluated by cluster of differentiation molecule 31 vessel staining, and proliferation (proliferating cell nuclear antigen staining) in response to both anti-VEGF treatments. These data demonstrate that the antiangiogenic approach was effective in inhibiting the growth of in situ dopamine-resistant prolactinomas as well as in the transplanted adenomas. No differences in VEGF protein expression were observed after either anti-VEGF treatment, and, although serum VEGF was increased in G6-31-treated mice, pituitary activation of the VEGF receptor 2 signaling pathway was reduced. Our results indicate that, even though the role of angiogenesis in pituitary adenomas is contentious, VEGF might contribute to adequate vascular supply and represent a supplementary therapeutic target in dopamine agonist-resistant prolactinomas.

Introduction

Prolactin-secreting adenomas are the most frequent type among pituitary tumors. Patients with prolactinoma usually present endocrinological symptoms resulting from hyperprolactinemia and, less commonly, visual defects caused by compression of the optic chiasm. Macroprolactinomas (tumor diameter >10 mm) are benign, slowly proliferating tumors, although they may be locally highly aggressive, particularly in males, and invade adjacent structures. Pharmacological therapy with dopamine agonists remains the mainstay of prolactinoma treatment, because dopamine D2 receptors (D2Rs) found in lactotropes inhibit cell proliferation and prolactin secretion (Ben-Jonathan and Hnasko, 2001). This therapy is effective in most patients, but 15% are resistant to classic dopamine agonist therapy. A decrease in number or function of D2Rs has been proposed in dopamine agonist resistance (Pellegrini et al., 1989; Caccavelli et al., 1996). In these cases, tumors tend to be invasive and aggressive and may require extirpation (Molitch, 2005). An alternative target would be desired in these circumstances.

This work was supported by the Consejo de Investigaciones Cientificas y Tecnicas [Grant PIP N-640, 2009] (to D.B.-V.); Agencia Nacional de Promoción Científica y Técnica (Buenos Aires, Argentina) [Grant PICT N-206, 2006] (to D.B.-V.); and the Fiorencio Fiorini.

Article, publication date, and citation information can be found at http://jpet.aspetjournals.org.

doi:10.1124/jpet.110.177790.

[S] The online version of this article (available at http://jpet.aspetjournals.org) contains supplemental material.

ABBREVIATIONS: D2R, dopamine D2 receptor; *Drd2*, D2R gene; *Drd2*(−/−), D2R knockout; mAb, monoclonal antibody; AKT, protein kinase B; pAKT, phosphorylated AKT; ANOVA, analysis of variance; BSA, bovine serum albumin; BW, body weight; CD31, cluster of differentiation molecule 31; VEGF, vascular endothelial growth factor; VEGFR2, VEGF receptor 2; Flt-1, VEGF receptor 1; VEGF-TRAP, mVEGF R1 (Flt-1)/Fc chimera; PBS, phosphate-buffered saline; PCNA, proliferating cell nuclear antigen; RIA, radioimmunoassay; α-SMA, α-smooth muscle actin; WT, wild type; SU5416, (3*Z*)-3-[(3,5-dimethyl-1*H*-pyrrol-2-yl)methylidene]-1,3-dihydro-2*H*-indol-2-one; TNP-470, *N*-(2-chloroacetyl)carbamic acid(3*R*,4*S*,5*S*,6*R*)-5-methoxy-4-[(2*R*,3*R*)-2-methyl-3-(3-methyl-2-buten-1-yl)-2-oxiranyl]-1-oxaspiro[2.5]oct-6-yl ester.

In most human tumors, including breast, bladder, and stomach, angiogenesis has been shown to be correlated with tumor behavior (Crawford and Ferrara, 2009). Development of new blood vessels provides tumor tissues with oxygen and basic energetic compounds (Folkman and Shing, 1992). On the other hand, the role of angiogenesis in pituitary tumor development has been questioned, because the normal pituitary is a highly vascularized gland, reflecting the need to respond to regulatory feedbacks and rapidly deliver hormones into circulation. Differences in the angiogenic pattern of pituitary tumors have yielded highly controversial results concerning hormonal phenotypes, size, or invasion (Turner et al., 2003; Di Ieva et al., 2008; Pizarro et al., 2009). Some data point to increased angiogenesis, whereas others have described that pituitary tumors are usually less vascularized than normal pituitary tissue (Schechter, 1972; Jugenburg et al., 1995; Turner et al., 2003).

Among angiogenic molecules, vascular endothelial growth factor (VEGF) has a central role. VEGF receptor 2 (VEGFR2) is the major positive signal transducer for both physiological and pathological angiogenesis induced by VEGF. It is a highly active kinase receptor and triggers a broad spectrum of signaling cascades. The phosphoinositide 3-kinase signal transduction pathway leading to phosphorylation of protein kinase B (AKT) has emerged as one of the main signal routes of VEGFR2 activation (Hoeben et al., 2004). Indeed, many experiments using in vivo and in vitro systems have demonstrated that activation of phosphoinositide 3-kinase by VEGFR2 promotes endothelial cell survival, proliferation, and angiogenesis, and the overexpression of a dominant-negative form of AKT blocked the survival effect of VEGF (Gerber et al., 1998).

The pituitary contains abundant VEGF as well as VEGFR2 (Ochoa et al., 2000; Vidal et al., 2002), and VEGF participates in the formation of the vascular network of a new pituitary tumor (Banerjee et al., 2000; Kim et al., 2005). It is also involved in the proliferative action of estrogen on lactotropes (Onofri et al., 2004), and increased tumoral VEGF expression was observed during estrogen-induced prolactinoma development in rats (Banerjee et al., 1997). These data indicate that, even though the role of angiogenesis in pituitary adenomas is contentious, VEGF might contribute to adequate temporal vascular supply.

We found increased VEGF expression in a cohort of dopamine-resistant prolactinomas (Cristina et al., 2010). Furthermore, a relationship between the D2R and endothelial cell proliferation within tumors has been proposed. Dopamine selectively inhibits VEGF-induced angiogenesis and inhibits the growth of malignant tumors, as well as the vascular permeabilizing and angiogenic activities of VEGF (Basu et al., 2001). In addition, in two outbred lines of Wistar rats, which present high and low dopaminergic reactivity, respectively, VEGF expression was lower in the first group, and this group was more resistant to tumor implantation and developed significantly fewer lung metastases (Teunis et al., 2002).

D2R knockout [*Drd2*(−/−)] mice, generated by targeted mutagenesis, have chronic hyperprolactinemia and pituitary hyperplasia and provide an experimental model for dopamine agonist-resistant prolactinomas (Cristina et al., 2006). In *Drd2*(−/−) mice highly vascularized adenomas develop after 16 months of age, especially in females, but also in males (Asa et al., 1999). Prominent vascular channels, as well as extravasated red blood cells not contained in capillaries or peliosis, are common findings in the hyperplastic and adenomatous *Drd2*(−/−) pituitaries. Peliosis has been found in different tumors that secrete VEGF. In accordance, VEGF mRNA and protein expression are increased in pituitaries from *Drd2*(−/−) female mice (Cristina et al., 2005). These results support the notion that the defective function of D2Rs increases VEGF expression and may participate in pituitary angiogenesis of prolactinomas.

Therefore, VEGF and its receptor may become supplementary therapeutic tools in dopamine agonist-resistant prolactinomas. To this regard, in recent years, blocking VEGF-mediated angiogenesis has been proposed as a novel alternative or a supplement to conventional cancer therapy, and a variety of regimens that prevent tumor angiogenesis and/or that attack tumor blood vessels have met with remarkable success in treating mouse cancers (Crawford and Ferrara, 2009).

To study the effect of blocking angiogenesis in prolactinoma development, we designed two experimental strategies using prolactinomas harbored by *Drd2*(−/−) female mice: direct intra-adenoma VEGF-TRAP injection in transplanted pituitaries and systemic VEGF neutralization. The aim of this study was to determine the effect of these antiangiogenic treatments in pituitary weight, prolactin content and secretion, adenoma proliferation index, and vasculature in the hyperplastic pituitaries.

Materials and Methods

Animals. C57BL/6J and *Drd2*(−/−) female mice were used. *Drd2*(−/−) mice [official strain designation B6;129S2-*Drd2*^{tm1low} by the Induced Mutant Resource at The Jackson Laboratory (Bar Harbor, ME)] were generated by targeted mutagenesis of the dopamine D2 receptor gene (*Drd2*) in embryonic stem cells (Kelly et al., 1997; Asa et al., 1999). The original F_2 hybrid strain (129S2/Sv × C57BL/6J) containing the mutated *Drd2* allele was backcrossed for at least 10 generations to wild-type (WT) C57BL/6J mice. Mutant and wild-type mice were the product of heterozygote crossings. Mice of mixed genotypes were housed in groups of four or five in a temperature-controlled room with lights on at 7:00 AM and lights off at 7:00 PM and free access to laboratory chow and tap water. All experimental procedures were reviewed and approved by the Institutional Animal Care and Use Committee of the Instituto de Biología y Medicina Experimental, Buenos Aires (Division of Animal Welfare, Office for Protection of Research Risks, National Institutes of Health).

Pituitary Transplantation and VEGF-TRAP Injection Protocol. Nine-month-old *Drd2*(−/−) female mice were decapitated, and removal of the hyperplastic pituitary was carried out under sterile conditions. Serum was kept for VEGF analysis by enzyme-linked immunosorbent assay. The excised pituitaries were placed in 5- to 7-mm-long silastic tubes of 1.2-mm inner diameter and 2.2-mm outer diameter (Dow Corning, Midland, MI), through an incision of 3 to 4 mm long, leaving both ends open. The silastic tubes were kept in saline solution for 1 h before surgery.

Six-month-old wild-type female mice were weighed and anesthetized by intraperitoneal injection of ketamine (80 mg/kg) plus xylazine (7 mg/kg). Each silastic tube containing one excised hyperplastic pituitary was then implanted subcutaneously in the left lateral flank of the wild-type mice. The surgical wound was closed, and the animals were kept warm until recovery. After implantation, animals were divided into two experimental groups: control (n = 7) and VEGF-TRAP-treated (n = 7). Treated animals received 2 μg of VEGF-TRAP (R&D Systems, Minneapolis, MN) in 20 μl of phosphate-buffered saline (PBS)/0.1% bovine serum albumin (BSA) per

injection twice a week for 3 weeks. Control animals received 20 μl of PBS and 0.1% BSA (vehicle). Injections were applied through the skin directly inside the implanted silastic tubes.

Every week blood was collected from the tail by snipping using a new scalpel blade; serum was separated and stored at −20°C until radioimmunoassays (RIAs) were performed.

On day 21, 1 day after the last injection, trunk blood was collected, and silastic tubes were rapidly and carefully removed. Pituitary grafts were isolated and cut into two parts. A big part of the graft was fixed by immersion in 10% buffered formalin and subsequently embedded in paraffin for immunohistochemistry, the other part was homogenized in ice-cold buffer containing 60 mM Tris-HCl, 1 mM EDTA, pH 6.8, and a mix of protease inhibitors [phenyl-methyl-sulfonyl, tosyl phenylalanyl chloromethyl ketone, *N*-α-(p-toluene sulfonyl)-L-arginine methyl ester, benzyloxycarbonyl-L-phenylalanine, and *N*-tosyl-L-lysine chloromethyl ketone] in a handheld microtissue homogenizer for prolactin measurement by RIA.

Monoclonal Antibody G6-31 Injection Protocol for In Situ Hyperplastic Pituitary Treatment. Five-month-old *Drd2*(−/−) female mice were intraperitoneally injected twice a week for 6 weeks with 5 mg/kg monoclonal antibody (mAb) G6-31 in PBS (mAb G6-31 group; $n = 7$) or PBS [*Drd2*(−/−) control group, $n = 7$; control wild-type group, $n = 6$]. Every 15 days blood samples were collected from the facial vein, and serum was separated and stored at −20°C until RIAs were performed. Once a week animals were weighed.

On day 43, all animals were decapitated, and pituitaries were carefully removed. A portion of the pituitary was homogenized in ice-cold buffer containing 60 mM Tris-HCl, 1 mM EDTA, pH 6.8, and a mix of proteases inhibitors in a handheld microtissue homogenizer for RIA or Western blot analysis. The other part was fixed by immersion in 10% buffered formalin and subsequently embedded in paraffin for immunohistochemistry. Weight of highly vascularized organs (spleen, liver, and kidney) was obtained on day 43. Serum was kept for prolactin and VEGF assays.

Drugs. The VEGF-TRAP used in these experiments comprises a portion of the extracellular domain of murine VEGF receptor type 1 (Flt-1) fused to the Fc portion of human IgG. This soluble truncated form of the Flt-1 receptor has been demonstrated to neutralize circulating VEGF and inhibit its action (Wulff et al., 2001). VEGF-TRAP was dissolved in PBS buffer with 0.1% BSA.

mAb G6-31 [anti-human and murine VEGF-A mAb kindly supplied by Genentech Inc., South San Francisco, CA (Liang et al., 2006)] was dissolved in PBS. All other reagents were purchased from Sigma-Aldrich (St. Louis, MO) unless otherwise specified.

RIA. Prolactin was measured by radioimmunoassay using mouse-specific reagents provided by the National Institute of Diabetes and Digestive and Kidney Diseases' National Hormone and Pituitary Program (Dr. A. F. Parlow, Torrance, CA). Assays were performed using 8 μl of serum in duplicate. Results are expressed in terms of mouse prolactin reference preparation 3. Intra-assay and interassay coefficients of variation were 7.2 and 12.8%, respectively.

VEGF Enzyme-Linked Immunosorbent Assay. Mouse serum VEGF concentrations were measured using the enzyme-linked immunoassay kit (Quantikine M Mouse VEGF; R&D Systems) following the manufacturer's instructions. Aliquots of 15 μl of serum were used in duplicate. The lower limit of the assay sensitivity was 7.8 pg/ml. The intra-assay coefficient of variation was 6.7%.

Immunohistochemistry. Pituitary sections were deparaffinized and hydrated in graded ethanols. A microwave pretreatment for antigen retrieval was performed in 10 mM sodium citrate buffer, pH 6. Endogenous peroxidase activity and nonspecific binding sites were blocked. Primary antibodies were incubated overnight at 4°C. After incubation with biotin-conjugated secondary antibodies for 1 h, the reactions were developed using a streptavidin-biotin peroxidase method and diaminobenzidine as a chromogen substrate. Samples were counterstained with hematoxylin and mounted with permanent mounting medium. Each immunohistochemical run included negative controls replacing the primary antibody with PBS. Antibodies used were rabbit polyclonal VEGF (1:200 and 1:100, for transplants or in situ pituitaries, respectively; Santa Cruz Biotechnologies Inc., Santa Cruz, CA), polyclonal antibody platelet endothelial cell adhesion molecule for cluster of differentiation molecule 31 (CD31) detection (1:400 and 1:100, for transplants or in situ pituitaries, respectively; Santa Cruz Biotechnologies Inc.), rabbit polyclonal anti-α-smooth muscle actin (α-SMA) (1:100; Abcam Inc., Cambridge, MA), rabbit polyclonal proliferating cell nuclear antigen (PCNA; 1:100; Santa Cruz Biotechnologies Inc.), and goat polyclonal antiprolactin (1:200; Santa Cruz Biotechnologies Inc.).

Western Blot. Pituitary samples were homogenized in 80 to 300 μl of ice-cold buffer containing 60 mM Tris-HCl, 1 mM EDTA, pH 6.8, and a mix of protease inhibitors [phenyl-methyl-sulfonile, tosyl phenylalanyl chloromethyl ketone, *N*-α-(p-toluene sulfonyl)-L-arginine methyl ester, benzyloxycarbonyl-L-phenylalanine, and *N*-tosyl-L-lysine chloromethyl ketone] in a handheld microtissue homogenizer. The homogenate was then centrifuged at 800*g* for 5 min at 4°C. An aliquot of supernatant was taken to quantify proteins by the Qubit Quant-it protein assay kit (Invitrogen, Buenos Aires, Argentina). Twenty two micrograms of proteins in 21 μl of homogenization buffer were mixed with 6 μl of 5× sample buffer (150 mM Tris-HCl, 10% SDS, 50% glycerol, 0.05% bromphenol blue, pH 6.8) and 3 μl of 10× dithiothreitol. Samples were heated 5 min at 95°C and subjected to 8% SDS-polyacrylamide gel electrophoresis. The gel was then blotted onto a nitrocellulose membrane and probed with the corresponding primary antibody followed by a secondary antibody conjugated with horseradish peroxidase. Polyclonal rabbit anti-pAKT (1:700; Cell Signaling, Danvers, MA), was used. AKT expression was evaluated to confirm equivalent total protein loading (1:1000; mouse anti-AKT; Abcam Inc.). For repeated immunoblotting, membranes were incubated in stripping buffer (1.5% glycine, 0.1% SDS, and 1% Tween 20, pH 2.2) for 10 min at room temperature and reprobed. Chemiluminescence was detected in a G:box chemi HR16 (Syngene, Frederick, MD). Band intensities were quantified using ImageJ software (National Institutes of Health, Bethesda, MD). Each pAKT band intensity was normalized to the respective AKT band intensity.

Quantification of Cell Proliferation. The PCNA labeling index was manually determined by counting brown-stained nuclei and expressed as percentage of cells showing unequivocal nuclear staining (positive nuclei × 100/total nuclei) in selected fields counterstained with hematoxylin dye. A mean of 30 fields each containing 100 cells was assessed per slide. Three slides per animals were counted.

Quantification of Vascular Areas. Evaluation of the relative vascular areas was carried out on sections immunostained with the CD31 antibody. Images of randomly selected fields of transplanted or in situ pituitaries were recorded using an Axiostar Plus microscope (Carl Zeiss Inc., Thornwood, NY) and a PowerShot G6 digital camera (Canon, Lake Success, NY), 40× or 100× objective, respectively. Microvessel density was calculated counting the number of CD31-positive vessels per square millimeter, and vascular area was determined by the cumulative area occupied by vessels expressed as percentage of area of vessels/total area. We also studied the size of vessels in the pituitary tumor samples in comparison with the control tissues. Three slides per pituitary were analyzed, and at least four images were counted per slide using the image processing and analysis software ImageJ (http://rsbweb.nih.gov/ij/).

The relative area occupied by mature vessels was calculated using sections immunostained with a pericyte marker, α-SMA; the relative area occupied by mature vessels, as well as the size and the number of vessels per area, were calculated as above.

Immunofluorescence and Confocal Laser Microscopy for In Situ Pituitaries. The antibody used was polyclonal goat antiprolactin (dilution 1:250; Santa Cruz Biotechnologies Inc.). After rinsing in PBS, the sections were incubated at room temperature for 90 min with anti-goat IgG fluorescein isothiocyanate (dilution 1:100; Vector Laboratories, Burlingame, CA). After rinsing in PBS, the sections were mounted in Vectashield (Vector Laboratories) to prevent fading

of the immunofluorescence reaction. Sections were examined on a C1 Plan Apo_60/1.4 oil confocal laser-scanning system (Nikon, Tokyo, Japan). The excitation wavelength was 488 nm for fluorescein isothiocyanate. Specificity studies were carried out by omitting primary antisera or preabsorbing primary antisera with homologous antigen excess; all showed the absence of the fluorescent signal.

Statistical Analyses. Results are expressed as means ± S.E.M. The differences between means were analyzed by analysis of variance (ANOVA) followed by Newman-Keuls test or Tukey's honestly significant difference test for unequal n [for pituitary prolactin content, percentage of lactotropes per area, quantification of immunohistochemistry (for PCNA, VEGF, CD31, and α-SMA); pAKT/AKT, serum VEGF levels and organ weights in mAb G6-31 treatment]. Two-way ANOVA with repeated-measures design was used to analyze body weight (BW) in mAb G6-31 treatment and serum prolactin levels in both treatments (effects of treatment and time). Two-way ANOVA was applied in PCNA, VEGF, CD31, and α-SMA quantification in VEGF-TRAP experiments (effects of treatment and tissue) and for serum VEGF concentration at two ages (effects of age and genotype). In all cases if F of interaction was found significant, individual means were compared by Fisher's protected least-significant difference tests; if it was not significant, groups of means were analyzed by the same test. Student's t test was used to analyze pituitary weight in mAb G6-31 experiments and prolactin tissue concentration and percentage of lactotropes in VEGF-TRAP experiments. $p < 0.05$ was considered significant.

Results

VEGF-TRAP Treatment of Transplanted Hyperplastic Pituitaries from *Drd2*(−/−) Female Mice. Hyperplastic pituitaries from 9-month-old *Drd2*(−/−) female mice were transplanted in silastic tubes in the flanks of wild-type female mice. After 3 weeks of local VEGF-TRAP injection into the silastic tubes, mice were decapitated and implants were removed. In the gross findings silastic grafts from vehicle-treated mice (controls) were highly vascularized and a diffuse reddish appearance was observed, whereas VEGF-TRAP-injected grafts were almost transparent with no evident signs of vascularization (Supplemental Fig. 1).

Prolactin Levels and Percentage of Lactotropes in VEGF-TRAP-Treated Pituitaries. Figure 1A shows that no significant differences were observed in serum prolactin levels between the control and VEGF-TRAP groups. In fact, serum prolactin was not significantly different in untransplanted (33.2 ± 10.8 ng/ml) compared with transplanted mice, indicating that the major component of circulating prolactin in this model was the in situ pituitary and not the graft. On the other hand, initial serum prolactin levels in both groups were higher than at the end of the treatment, which may be related to the fact that the last samples were obtained by decapitation and not from the tail, a procedure that may involve stress.

In the excised transplants, prolactin concentration (ng/μg protein) and percentage of lactotropes in the total tissue were reduced in VEGF-TRAP-treated compared with vehicle-treated transplants (Fig. 1, B and C; $p = 0.049$, and 0.023, respectively).

Cellular Proliferation and VEGF Protein Expression in VEGF-TRAP-Treated Pituitaries. Each pituitary graft had endocrine tissue that was prolactin-immunopositive and nonendocrine tissue that comprised the rest of the transplant.

To assess the extent of proliferation in the transplanted pituitaries and nonendocrine tissue of the transplants, an immunohistochemical staining with PCNA antibody was performed. Two-way ANOVA indicated that PCNA labeling index was significantly reduced by VEGF-TRAP treatment in endocrine and nonendocrine tissue [Fig. 2A and Supplemental Fig. 2, A and B; p interaction (group × tissue) = 0.22; p treatment = 0.0010].

VEGF immunopositivity was localized mainly within the cytoplasm, and there was also minor nuclear staining. The area occupied by VEGF-immunopositive cells was similar in both treatment groups, endocrine and nonendocrine tissue (Fig. 2B).

Microvascular Density in VEGF-TRAP-Treated Pituitaries. To test the efficacy of anti-VEGF treatment in inhibiting angiogenesis in the pituitary adenoma grafts, vascular area and density of vessels were analyzed by immunohistochemical staining with CD31, an endothelial cell marker. Vascular area and the number of CD31-positive vessels per area were decreased in VEGF-TRAP-treated compared with vehicle-treated pituitary transplants, both in the endocrine and nonendocrine tissue [Fig. 3, A and B; interaction (group × tissue) was not significant in both measurements, and $p = 0.0041$ and 0.013 for the effect of treatment on the vascular area and vessel density, respectively]. Vessel size was not modified by treatment (Fig. 3C).

On the other hand, no significant differences were observed in α-SMA-positive vessels or the vascular area between the VEGF-TRAP and vehicle treatment groups (Fig. 4).

Taking into account these results obtained with locally injected VEGF-TRAP, we decided to test a systemic anti-VEGF treatment with mAb G6-31, which could represent a better preclinical model.

Effect of Systemic mAb G6-31 Treatment on Pituitary Weight and Prolactin Levels in *Drd2*(−/−) Female Mice. Treatment with anti-VEGF-A mAb G6-31, which

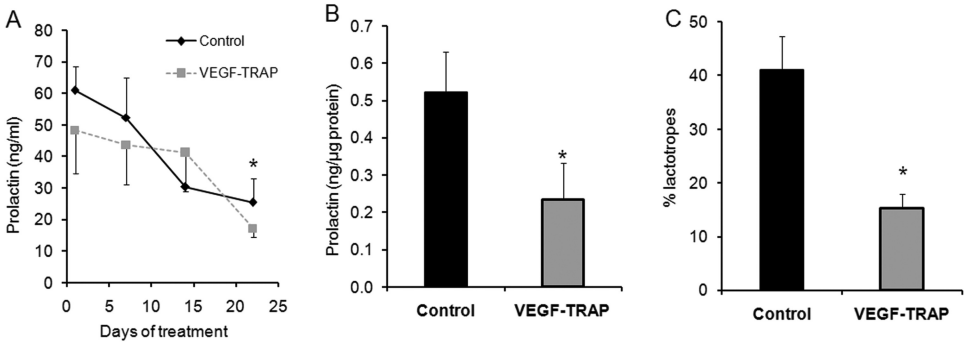

Fig. 1. A, serum prolactin levels (ng/ml) in female mice harboring *Drd2*(−/−)-transplanted pituitaries in the flank and treated locally with vehicle (control; $n = 7$) and VEGF-TRAP ($n = 7$) are shown. Mean and S.E.M. values are depicted. *, $p < 0.05$ versus treatment-matched time 0. B, prolactin concentration (ng/μg protein) in control ($n = 6$) and VEGF-TRAP-treated transplants ($n = 7$) is shown. *, $p < 0.05$. C, percentage of prolactin-positive cells by immunohistochemistry in control ($n = 7$) and VEGF-TRAP-treated ($n = 7$) whole grafts is shown. *, $p < 0.05$.

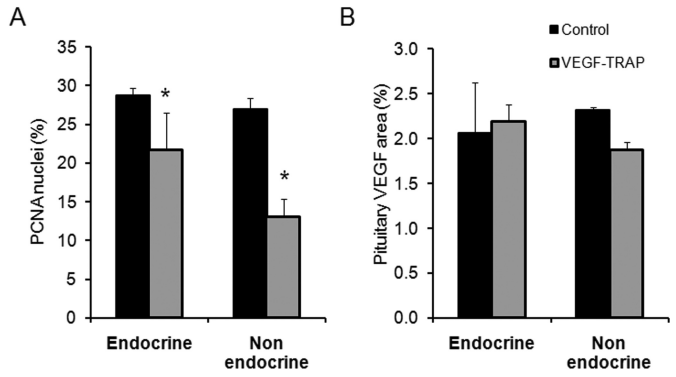

Fig. 2. A, percentage of positive PCNA-stained cells (positive PCNA nuclei × 100/total nuclei) in the endocrine and nonendocrine tissue in control ($n = 5$) or VEGF-TRAP-treated ($n = 4$) grafts is shown. *, $p < 0.05$ versus tissue-matched control. B, percentage of VEGF-stained area (VEGF-stained area × 100/whole area) in the endocrine and nonendocrine tissue in control ($n = 5$) or VEGF-TRAP-treated ($n = 4$) grafts is shown.

binds both human and murine VEGF with high affinity, significantly reduced pituitary weight in *Drd2*(−/−) mice (Fig. 5A; $p = 0.036$).

Prolactin Levels and Area Occupied by Prolactin-Positive Cells in mAb G6-31-Treated Pituitaries. There were no differences in serum prolactin levels between experimental groups throughout treatment (Fig. 5B); however, pituitary prolactin content (ng/gland) (Fig. 5C) and the area occupied by prolactin-positive cells (Fig. 5D) were decreased in pituitaries from *Drd2*(−/−) mice treated with mAb G6-31 [$p = 0.010$ and 0.0045, for prolactin content and prolactin-positive area, respectively, *Drd2*(−/−) control versus *Drd2*(−/−) mAb G6-31-treated group].

Cellular Proliferation in mAb G6-31-Treated Pituitaries. Quantitative analysis of PCNA labeling index revealed a marked decrease in PCNA-positive cells in hyperplastic pituitaries of *Drd2*(−/−) mice treated with mAb G6-31 compared with the vehicle-treated group (Fig. 6; $p = 0.0080$; and Supplemental Fig. 2, C and D). The PCNA index in mAb G6-31-treated pituitaries was similar to that in pituitaries from wild-type female mice. Comparing PCNA labeling index in both models, we observed a lower PCNA index in in situ *Drd2*(−/−) pituitaries compared with pituitary transplants (Figs. 2A and 6).

Serum VEGF, Pituitary VEGF, and Phosphorylated AKT/AKT in mAb G6-31-Treated Pituitaries. On the other hand, a similar VEGF-positive immunohistochemical area was found in hyperplastic pituitaries from *Drd2*(−/−) mice treated with PBS or mAb G6-31 (Fig. 7A). Serum VEGF was significantly increased in 5- and 9-month-old *Drd2*(−/−) mice compared with wild-type age-matched mice (Fig. 7B; $p = 0.012$ for the genotype effect), and mAb G6-31 treatment further increased serum VEGF levels in *Drd2*(−/−) mice [Fig. 7C; $p < 0.0001$, mAb G631 *Drd2*(−/−) versus untreated *Drd2*(−/−) or wild-type mice]. Nevertheless, the VEGF signal transduction pathway leading to phosphorylation of AKT was decreased in pituitaries from mAb G6-31-treated mice, compared with pituitaries from untreated mice ($p = 0.0028$; Fig. 7D), indicating an effective sequestering of VEGF.

Microvascular Area and Density in mAb G6-31-Treated Pituitaries. Quantification of vessel density indicated that the vascular component of pituitaries from mAb G6-31-treated mice was significantly reduced compared with that in vehicle-treated mice. Pituitary CD31 vascular area and the number of CD31-positive vessels per area were decreased in *Drd2*(−/−) mAb G6-31-treated mice compared with the *Drd2*(−/−) vehicle-treated group (Fig. 8, A and B; $p = 0.0090$ and 0.0028 for area and density, respectively) and achieved similar levels to those of pituitaries from wild-type mice [$p = 0.57$ and 0.33 for area and density; *Drd2*(−/−) mAb G6-31-treated versus wild-type pituitaries]. On the other hand, no differences in average vessel size were detected among groups (Fig. 8C). Comparing both experimental mod-

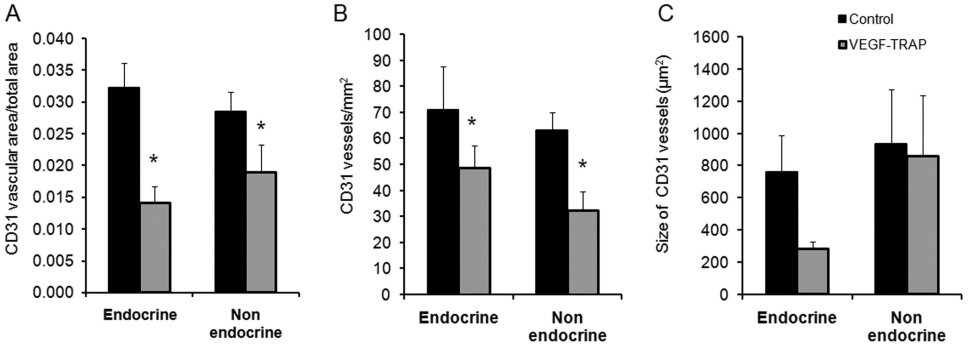

Fig. 3. A, relative CD31-stained vascular area (CD 31 vascular area/total area) in the endocrine ($n = 6$ and 4) and nonendocrine tissue ($n = 6$ and 5) in control or VEGF-TRAP-treated grafts is shown. B, vessel density (number of CD31-stained vessels/mm^2) in the endocrine and nonendocrine tissue, in control or VEGF-TRAP-treated grafts. *, $p < 0.05$ versus tissue-matched control. C, average size (µm^2) of CD31-positive vessels in the endocrine and nonendocrine tissue is shown in control or VEGF-TRAP-treated grafts.

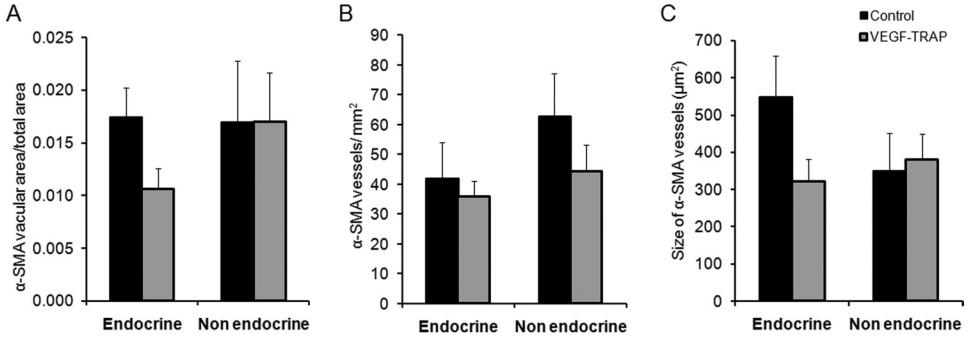

Fig. 4. A, relative α-SMA-stained area (positive α-SMA vascular area/total area) in the endocrine and nonendocrine tissue in control ($n = 5$) or VEGF-TRAP-treated ($n = 5$) grafts is shown. B, vessel density (number of α-SMA-stained vessels/mm^2) in the endocrine and nonendocrine tissue in control or VEGF-TRAP-treated grafts is shown. C, average size (µm^2) of α-SMA-positive vessels in the endocrine and nonendocrine tissue in control or VEGF-TRAP-treated grafts is shown.

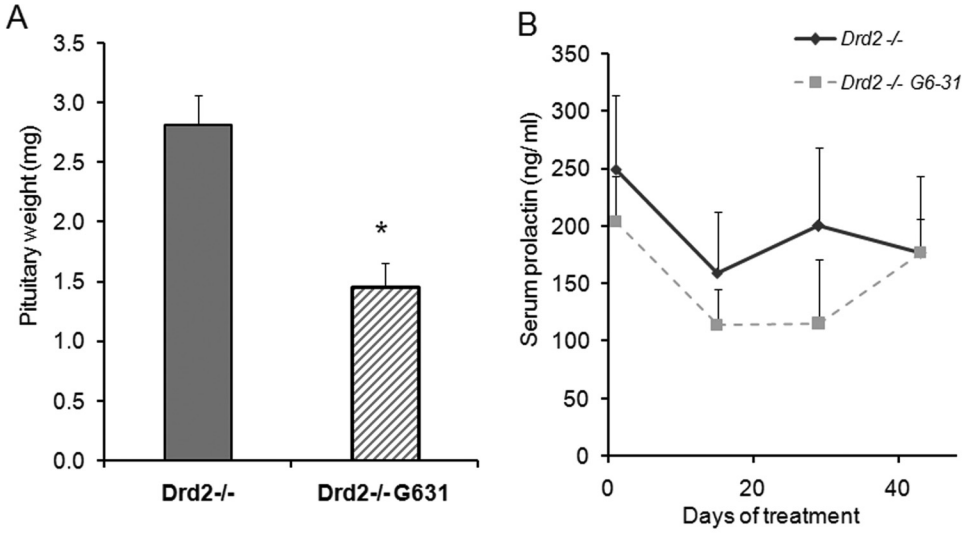

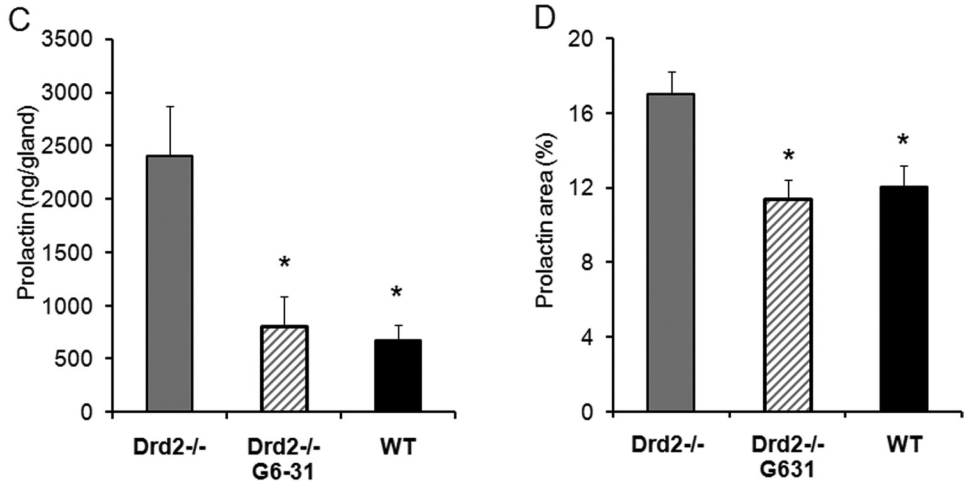

Fig. 5. A, pituitary weight is shown in vehicle ($n = 5$) and mAb G6-31-treated ($n = 7$) *Drd2*(−/−) female mice. ∗, $p < 0.05$ versus vehicle and *Drd2*(−/−)-treated mice. B, serum prolactin levels are shown in female *Drd2*(−/−) vehicle ($n = 5$) or *Drd2*(−/−) mAb G6-31-treated ($n = 7$) mice. C, pituitary prolactin concentration (ng/gland) in control *Drd2*(−/−), mAb G6-31-treated *Drd2*(−/−), and WT female mice ($n = 5$ for all) is shown. D, percentage of prolactin-positive area by confocal immunohistochemistry in control *Drd2*(−/−) ($n = 6$), mAb G6-31-treated *Drd2*(−/−) ($n = 7$), and WT female ($n = 5$) mice is shown. ∗, $p < 0.05$ versus *Drd2*(−/−) vehicle-treated mice.

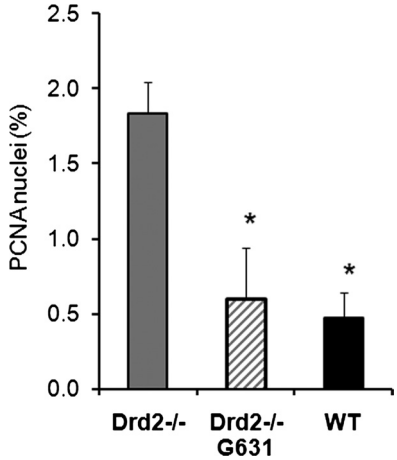

Fig. 6. Percentage of PCNA-stained cells (positive PCNA nuclei × 100/total nuclei) was evaluated by immunohistochemistry in control *Drd2*(−/−) ($n = 6$), mAb G6-31-treated *Drd2*(−/−) ($n = 6$), and WT female ($n = 4$) mice. ∗, $p < 0.05$ versus *Drd2*(−/−) vehicle-treated mice.

els we observed that in situ pituitaries had a higher proportion of small vessels (average size 10 μm^2) compared with the pituitary transplants that had fewer vessels, but their average size was bigger (see Figs. 4 and 8).

When immunohistochemical analysis was performed using staining with anti-α-SMA (a marker of mature vessels), no significant differences were encountered between the groups (Fig. 9).

Mice treated with the inhibitor of VEGF signaling were healthy, and none died during the treatment. BW was not different between treatment groups at any period, but two-way ANOVA revealed that mAb G6-31 mice had lower weight at 29, 36, and 43 days compared with initial BW, whereas no differences were detected in the vehicle-treated group [p interaction time × treatment (6,60) = 0.036, and $p < 0.005$ for BW on days 29, 36, and 43 versus initial BW]. Pancreas, liver, kidney, and spleen weights at the end of the treatment were similar between groups (Supplemental Fig. 3).

Discussion

There has been great interest in the targeting of tumor vasculature and the development of antiangiogenic agents, which interrupt tumor's supply of oxygen and nutrients. Treatment with anti-VEGF antibodies significantly inhibited the growth of several tumor cells lines and has been approved by the Food and Drug Administration for combinatorial treatment with chemotherapy for metastatic colorectal cancer, non–small-cell lung cancer, metastatic breast cancer, and glioblastoma multiforme and renal cell carcinoma (Ferrara, 2010). However, not all trials have been positive (Burris

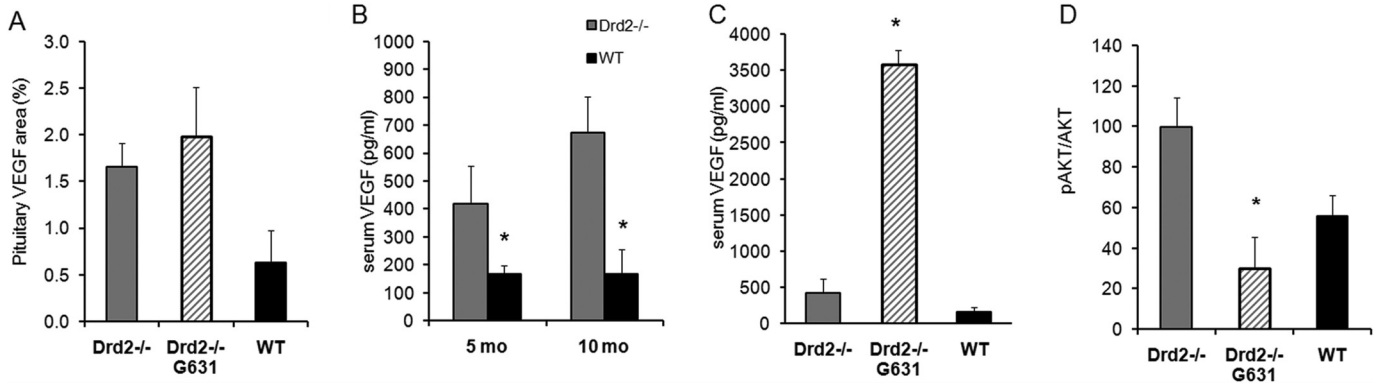

Fig. 7. A, percentage of VEGF-stained area (VEGF-stained area × 100/whole area) in control *Drd2*(−/−) (n = 3), mAb G6-31-treated *Drd2*(−/−) (n = 6), and WT female (n = 3) mice is shown. B, serum VEGF (pg/ml) in 5- and 9-month-old *Drd2*(−/−) (n = 5 and 7, respectively) and WT female mice (n = 6 and 7, respectively) mice is shown. *, $p < 0.05$ versus *Drd2*(−/−) mice. C, serum VEGF (pg/ml) in control *Drd2*(−/−) (n = 5), mAb G6-31-treated *Drd2*(−/−) (n = 7), and WT female (n = 6) mice is shown. *, $p < 0.05$ versus *Drd2*(−/−) vehicle-treated mice. D, pAKT/AKT (Western blot) in control *Drd2*(−/−) (n = 4), mAb G6-31-treated *Drd2*(−/−) (n = 5), and WT female (n = 5) mice is shown. *, $p < 0.05$ versus *Drd2*(−/−) vehicle-treated mice.

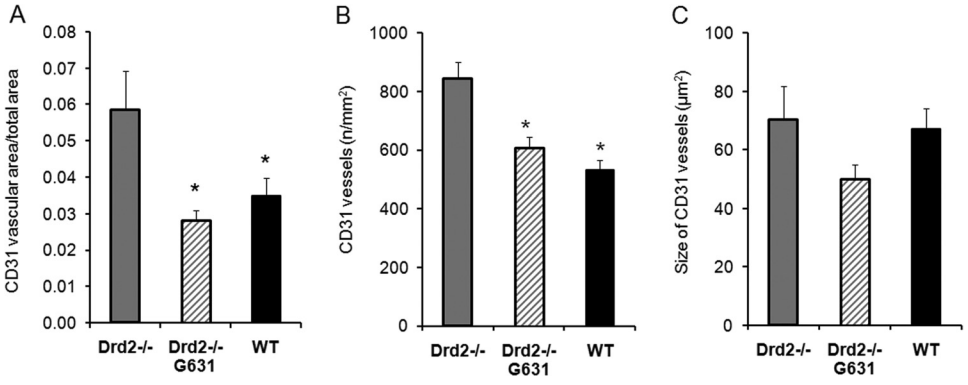

Fig. 8. A, relative CD31-stained vascular area (CD31 vascular area/total area) in control *Drd2*(−/−) (n = 5), mAb G6-31-treated *Drd2*(−/−) (n = 6), and WT female (n = 4) mice is shown. B, vessel density (number of CD31-stained vessels/mm^2) in control *Drd2*(−/−) (n = 5), mAb G6-31-treated *Drd2*(−/−) (n = 6), and WT female (n = 4) mice is shown. C, average size (μm^2) of CD31-positive vessels in control *Drd2*(−/−) (n = 5), mAb G6-31-treated *Drd2*(−/−) (n = 6), and WT female (n = 4) mice is shown. *, $p <$ 0.05 versus *Drd2*(−/−) vehicle-treated mice.

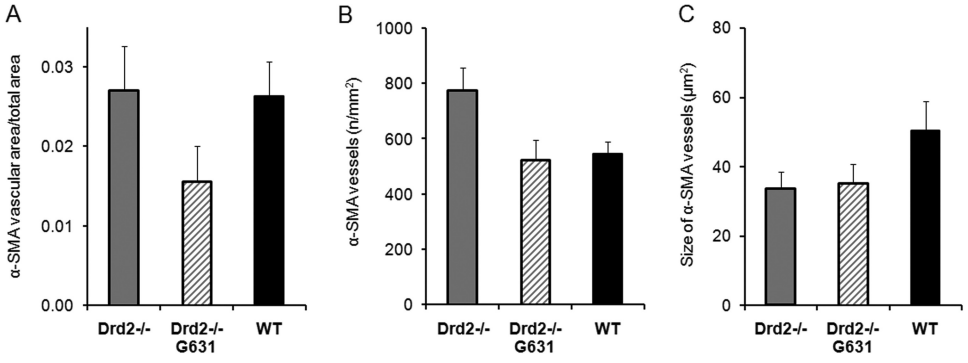

Fig. 9. A, relative α-SMA-stained area (α-SMA vascular area/total area) in control *Drd2*(−/−) (n = 6), mAb G6-31-treated *Drd2*(−/−) (n = 6), and WT female (n = 4) mice is shown. B, vessel density [number of α-SMA-stained vessels/area (mm^2)] in control *Drd2*(−/−) (n = 6), mAb G6-31-treated *Drd2*(−/−) (n = 6), and WT female (n = 4) mice is shown. C, average size (μm^2) of α-SMA-positive vessels in control *Drd2*(−/−) (n = 6), mAb G6-31-treated *Drd2*(−/−) (n = 6), and WT female (n = 4) mice is shown.

and Rocha-Lima, 2008; Kerbel, 2008), indicating that individual characteristics of different tumors should be studied. In particular, the effect of anti-VEGF therapy on endocrine or benign tumors has not been reported in clinical practice.

The role of angiogenesis in pituitary adenoma generation has been questioned, and furthermore there are no data of anti-VEGF strategies in dopamine agonist-resistant prolactinomas, even though these tumors have faulty D2Rs, and D2Rs have been linked to VEGF expression in other tumors (Caccavelli et al., 1996; Basu et al., 2001). Using two strategies with anti-VEGF compounds we demonstrate that VEGF is required for the maximal growth of a mouse model of dopamine agonist-resistant prolactinomas. Local therapy with VEGF-TRAP or a systemic treatment with a monoclonal antibody targeting murine VEGF resulted in substantial tumor and prolactin inhibition in hyperplastic pituitaries from *Drd2*(−/−) female mice. In addition, there were significant decreases in vascularization and proliferation index induced by both anti-VEGF strategies in the pituitary tumors. These data suggest that the antiangiogenic treatments were effective in inhibiting the growth of primary dopamine-resistant prolactinomas as well as the transplanted adenomas.

When we compared both models [grafted and in situ hyperplastic pituitaries from *Drd2*(−/−) female mice] we observed a different pattern of vascularization and proliferation index. In in situ pituitaries many small vessels and a low PCNA index were observed, whereas the pituitary transplants had fewer vessels, but their average size was bigger, and the PCNA index was higher. This probably reflects the adaptation of vascularization and cellular proliferation of the active transplanted tissue in a different environment.

Even though vascularization was decreased there were no differences in pituitary VEGF protein expression after either anti-VEGF treatment. But during mAb G6-31 treatment se-

rum VEGF levels markedly rose. This is in accordance with the results of several anti-VEGF treatments that show that VEGF expression increases by different antiangiogenic treatments (Wulff et al., 2001; Batchelor et al., 2007; Korsisaari et al., 2008). High-serum VEGF expression after anti-VEGF treatment may be the result of a compensatory mechanism to the sequestering of VEGF. Nevertheless, in our experimental model VEGFR signaling pathway was reduced by the treatment, as shown by a decrease in phosphorylated AKT in in situ pituitaries from *Drd2*(−/−) mice treated with mAb G6-31, probably indicating an effective neutralization of VEGF action.

α-SMA-positive vessels indicate the presence of pericytes and therefore a greater degree of maturation or stabilization of the vasculature. α-SMA vessels were present in pituitaries of both models, but the anti-VEGF treatment did not lower this component. This may be related to the fact that VEGF is acting on proliferation of endothelial cells and not on pericytes, which may be the source of VEGF but not the target as described during the angiogenesis of the corpus luteum (Reynolds et al., 2000). These α-SMA-positive cells could be acting in a paracrine and cell-to-cell contact control of growth and differentiation of the endothelium.

We were surprised to find that mAb G6-31 lowered body weight after 3 weeks of treatment. Even though loss of body weight is not a common finding in different anti-VEGF experimental treatments, it has been described that treatment with (3*Z*)-3-[(3,5-dimethyl-1*H*-pyrrol-2-yl)methylidene]-1,3-dihydro-2*H*-indol-2-one (SU5416), a potent and selective inhibitor of VEGFR2, resulted in a transient body weight loss in mice after the first 7 days of administration (Fong et al., 1999), and a high dose (100 mg/kg) of *N*-(2-chloroacetyl)carbamic acid(3*R*,4*S*,5*S*,6*R*)-5-methoxy-4-[(2*R*,3*R*)-2-methyl-3-(3-methyl-2-buten-1-yl)-2-oxiranyl]-1-oxaspiro[2.5]oct-6-yl ester (TNP-470), an angiogenesis inhibitor, resulted in a severe reduction of body weight in nude mice (Mori et al., 2000).

Several lines of evidence indicated that VEGF could participate in pituitary adenoma generation. The VEGF system plays a crucial role in the regulation of tumor angiogenesis during the development of estrogen-induced prolactin-secreting pituitary tumors (Banerjee et al., 1997), and increased concentrations of VEGF and the VEGFR2 have been reported in these rat pituitary tumors (Banerjee et al., 1997). Nevertheless, VEGF increase in these models is ascribed to the action of estrogen, but *Drd2*(−/−) female mice (Cristina et al., 2005) and humans with prolactinomas are hypoestrogenic. In human studies VEGF expression in pituitary adenomas has yielded inconclusive results (Lloyd et al., 1999; McCabe et al., 2002), even though elevated serum VEGF concentrations have been demonstrated in some patients harboring pituitary tumors (Komorowski et al., 2000), and approximately 90% of human pituitary tumors cultured in vitro show measurable VEGF secretion (Lohrer et al., 2001).

Our previous data indicated that the lack of or defective D2R signaling in mice pituitaries leads to prolactinoma generation in correlation with increased pituitary VEGF expression in females (Cristina et al., 2005). Accordingly, we now show that serum VEGF was increased in *Drd2*(−/−) female mice. Furthermore, in human pituitary adenomas we found that VEGF protein expression was higher in dopamine-resistant prolactinomas compared with nonfunctioning growth hormone or adrenocorticotropic hormone-secreting adenomas, and the strong positive association of VEGF and CD31 expression found in these prolactinomas suggested the participation of tumor vascularization in adenoma development (Cristina et al., 2010). Furthermore, in an aggressive prolactinoma generated in the multiple endocrine neoplasia 1 mouse model mAb G6-31 inhibited the growth of the intracerebrally injected pituitary adenoma and reduced prolactin levels (Korsisaari et al., 2008).

Therefore, our present and previous results indicate that even though the role of angiogenesis in pituitary adenomas is controversial, VEGF might contribute to adequate temporal vascular supply and represent a complementary therapeutic target in aggressive dopamine agonist resistant prolactinomas. Tumor angiogenesis in the pituitary, as well as in other endocrine neoplasms, probably reflects the basic observation that tumors require neovascularization to grow; however, the changes that occur may be somewhat different from some other tissues that are less highly vascularized in the non-neoplastic state.

Acknowledgments

We thank the National Institute of Diabetes and Digestive and Kidney Diseases' National Hormone and Pituitary Program and Dr. A. F. Parlow for prolactin RIA kits and Genentech for mAb G6-31 (anti-human and murine VEGF-A monoclonal antibody).

Authorship Contributions

Participated in research design: Luque, Cristina, and Becu-Villalobos.
Conducted experiments: Luque, Perez-Millan, Ornstein, and Cristina.
Performed data analysis: Luque and Becu-Villalobos.
Wrote or contributed to the writing of the manuscript: Luque, Perez-Millan, Cristina, and Becu-Villalobos.

References

Asa SL, Kelly MA, Grandy DK, and Low MJ (1999) Pituitary lactotroph adenomas develop after prolonged lactotroph hyperplasia in dopamine D2 receptor-deficient mice. *Endocrinology* **140:**5348–5355.
Banerjee SK, Sarkar DK, Weston AP, De A, and Campbell DR (1997) Overexpression of vascular endothelial growth factor and its receptor during the development of estrogen-induced rat pituitary tumors may mediate estrogen-initiated tumor angiogenesis. *Carcinogenesis* **18:**1155–1161.
Banerjee SK, Zoubine MN, Tran TM, Weston AP, and Campbell DR (2000) Overexpression of vascular endothelial growth factor164 and its co-receptor neuropilin-1 in estrogen-induced rat pituitary tumors and GH3 rat pituitary tumor cells. *Int J Oncol* **16:**253–260.
Basu S, Nagy JA, Pal S, Vasile E, Eckelhoefer IA, Bliss VS, Manseau EJ, Dasgupta PS, Dvorak HF, and Mukhopadhyay D (2001) The neurotransmitter dopamine inhibits angiogenesis induced by vascular permeability factor/vascular endothelial growth factor. *Nat Med* **7:**569–574.
Batchelor TT, Sorensen AG, di Tomaso E, Zhang WT, Duda DG, Cohen KS, Kozak KR, Cahill DP, Chen PJ, Zhu M, et al. (2007) AZD2171, a pan-VEGF receptor tyrosine kinase inhibitor, normalizes tumor vasculature and alleviates edema in glioblastoma patients. *Cancer Cell* **11:**83–95.
Ben-Jonathan N and Hnasko R (2001) Dopamine as a prolactin (PRL) inhibitor. *Endocr Rev* **22:**724–763.
Burris H 3rd and Rocha-Lima C (2008) New therapeutic directions for advanced pancreatic cancer: targeting the epidermal growth factor and vascular endothelial growth factor pathways. *Oncologist* **13:**289–298.
Caccavelli L, Morange-Ramos I, Kordon C, Jaquet P, and Enjalbert A (1996) Alteration of Gα subunits mRNA levels in bromocriptine resistant prolactinomas. *J Neuroendocrinol* **8:**737–746.
Crawford Y and Ferrara N (2009) VEGF inhibition: insights from preclinical and clinical studies. *Cell Tissue Res* **335:**261–269.
Cristina C, Díaz-Torga G, Baldi A, Góngora A, Rubinstein M, Low MJ, and Becú-Villalobos D (2005) Increased pituitary vascular endothelial growth factor-a in dopaminergic D2 receptor knockout female mice. *Endocrinology* **146:**2952–2962.
Cristina C, García-Tornadú I, Díaz-Torga G, Rubinstein M, Low MJ, and Becú-Villalobos D (2006) Dopaminergic D2 receptor knockout mouse: an animal model of prolactinoma. *Front Horm Res* **35:**50–63.
Cristina C, Perez-Millan MI, Luque G, Dulce RA, Sevlever G, Berner SI, and Becu-Villalobos D (2010) VEGF and CD31 association in pituitary adenomas. *Endocr Pathol* **21:**154–160.
Di Ieva A, Grizzi F, Gaetani P, Goglia U, Tschabitscher M, Mortini P, and Rodriguez y Baena R (2008) Euclidean and fractal geometry of microvascular networks in normal and neoplastic pituitary tissue. *Neurosurg Rev* **31:**271–281.

Ferrara N (2010) Pathways mediating VEGF-independent tumor angiogenesis. *Cytokine Growth Factor Rev* **21:**21–26.
Folkman J and Shing Y (1992) Angiogenesis. *J Biol Chem* **267:**10931–10934.
Fong TA, Shawver LK, Sun L, Tang C, App H, Powell TJ, Kim YH, Schreck R, Wang X, Risau W, et al. (1999) SU5416 is a potent and selective inhibitor of the vascular endothelial growth factor receptor (Flk-1/KDR) that inhibits tyrosine kinase catalysis, tumor vascularization, and growth of multiple tumor types. *Cancer Res* **59:**99–106.
Gerber HP, McMurtrey A, Kowalski J, Yan M, Keyt BA, Dixit V, and Ferrara N (1998) Vascular endothelial growth factor regulates endothelial cell survival through the phosphatidylinositol 3′-kinase/Akt signal transduction pathway. Requirement for Flk-1/KDR activation. *J Biol Chem* **273:**30336–30343.
Hoeben A, Landuyt B, Highley MS, Wildiers H, Van Oosterom AT, and De Bruijn EA (2004) Vascular endothelial growth factor and angiogenesis. *Pharmacol Rev* **56:** 549–580.
Jugenburg M, Kovacs K, Stefaneanu L, and Scheithauer BW (1995) Vasculature in nontumorous hypophyses, pituitary adenomas, and carcinomas: a quantitative morphologic study. *Endocr Pathol* **6:**115–124.
Kelly MA, Rubinstein M, Asa SL, Zhang G, Saez C, Bunzow JR, Allen RG, Hnasko R, Ben-Jonathan N, Grandy DK, et al. (1997) Pituitary lactotroph hyperplasia and chronic hyperprolactinemia in dopamine D2 receptor-deficient mice. *Neuron* **19:** 103–113.
Kerbel RS (2008) Tumor angiogenesis. *N Engl J Med* **358:**2039–2049.
Kim K, Yoshida D, and Teramoto A (2005) Expression of hypoxia-inducible factor 1α and vascular endothelial growth factor in pituitary adenomas. *Endocr Pathol* **16:**115–121.
Komorowski J, Jankewicz J, and Stepień H (2000) Vascular endothelial growth factor (VEGF), basic fibroblast growth factor (bFGF) and soluble interleukin-2 receptor (sIL-2R) concentrations in peripheral blood as markers of pituitary tumours. *Cytobios* **101:**151–159.
Korsisaari N, Ross J, Wu X, Kowanetz M, Pal N, Hall L, Eastham-Anderson J, Forrest WF, Van Bruggen N, Peale FV, et al. (2008) Blocking vascular endothelial growth factor-A inhibits the growth of pituitary adenomas and lowers serum prolactin level in a mouse model of multiple endocrine neoplasia type 1. *Clin Cancer Res* **14:**249–258.
Liang WC, Wu X, Peale FV, Lee CV, Meng YG, Gutierrez J, Fu L, Malik AK, Gerber HP, Ferrara N, et al. (2006) Cross-species vascular endothelial growth factor (VEGF)-blocking antibodies completely inhibit the growth of human tumor xenografts and measure the contribution of stromal VEGF. *J Biol Chem* **281:**951–961.
Lloyd RV, Scheithauer BW, Kuroki T, Vidal S, Kovacs K, and Stefaneanu L (1999) Vascular endothelial growth factor (VEGF) expression in human pituitary adenomas and carcinomas. *Endocr Pathol* **10:**229–235.
Lohrer P, Gloddek J, Hopfner U, Losa M, Uhl E, Pagotto U, Stalla GK, and Renner U (2001) Vascular endothelial growth factor production and regulation in rodent and human pituitary tumor cells in vitro. *Neuroendocrinology* **74:**95–105.
McCabe CJ, Boelaert K, Tannahill LA, Heaney AP, Stratford AL, Khaira JS, Hussain S, Sheppard MC, Franklyn JA, and Gittoes NJ (2002) Vascular endothelial growth factor, its receptor KDR/Flk-1, and pituitary tumor transforming gene in pituitary tumors. *J Clin Endocrinol Metab* **87:**4238–4244.
Molitch ME (2005) Pharmacologic resistance in prolactinoma patients. *Pituitary* **8:**43–52.
Mori J, Haisa M, Naomoto Y, Takaoka M, Kimura M, Yamatsuji T, Notohara K, and Tanaka N (2000) Suppression of tumor growth and downregulation of platelet-derived endothelial cell growth factor/thymidine phosphorylase in tumor cells by angiogenesis inhibitor TNP-470. *Jpn J Cancer Res* **91:**643–650.
Ochoa AL, Mitchner NA, Paynter CD, Morris RE, and Ben-Jonathan N (2000) Vascular endothelial growth factor in the rat pituitary: differential distribution and regulation by estrogen. *J. Endocrinol* **165:**483–492.
Onofri C, Carbia Nagashima A, Schaaf L, Feirer M, Lohrer P, Stummer W, Berner S, Chervin A, Goldberg V, Stalla GK, et al. (2004) Estradiol stimulates vascular endothelial growth factor and interleukin-6 in human lactotroph and lactosomatotroph pituitary adenomas. *Exp Clin Endocrinol Diabetes* **112:**18–23.
Pellegrini I, Rasolonjanahary R, Gunz G, Bertrand P, Delivet S, Jedynak CP, Kordon C, Peillon F, Jaquet P, and Enjalbert A (1989) Resistance to bromocriptine in prolactinomas. *J Clin Endocrinol Metab* **69:**500–509.
Pizarro CB, Oliveira MC, Pereira-Lima JF, Leães CG, Kramer CK, Schuch T, Barbosa-Coutinho LM, and Ferreira NP (2009) Evaluation of angiogenesis in 77 pituitary adenomas using endoglin as a marker. *Neuropathology* **29:**40–44.
Reynolds LP, Grazul-Bilska AT, and Redmer DA (2000) Angiogenesis in the corpus luteum. *Endocrine* **12:**1–9.
Schechter J (1972) Ultrastructural changes in the capillary bed of human pituitary tumors. *Am J Pathol* **67:**109–126.
Teunis MA, Kavelaars A, Voest E, Bakker JM, Ellenbroek BA, Cools AR, and Heijnen CJ (2002) Reduced tumor growth, experimental metastasis formation, and angiogenesis in rats with a hyperreactive dopaminergic system. *FASEB J* **16:** 1465–1467.
Turner HE, Harris AL, Melmed S, and Wass JA (2003) Angiogenesis in endocrine tumors. *Endocr Rev* **24:**600–632.
Vidal S, Lloyd RV, Moya L, Scheithauer BW, and Kovacs K (2002) Expression and distribution of vascular endothelial growth factor receptor Flk-1 in the rat pituitary. *J Histochem Cytochem* **50:**533–540.
Wulff C, Wiegand SJ, Saunders PT, Scobie GA, and Fraser HM (2001) Angiogenesis during follicular development in the primate and its inhibition by treatment with truncated Flt-1-Fc (vascular endothelial growth factor Trap(A40)). *Endocrinology* **142:**3244–3254.

Address correspondence to: Damasia Becu-Villalobos, Instituto de Biología y Medicina Experimental-CONICET, Vuelta de Obligado 2490, Buenos Aires 1428, Argentina. E-mail dbecu@ibyme.conicet.org.ar